The Journal of Infectious Diseases

MAJOR ARTICLE

CD-loop Extension in Zika Virus Envelope Protein Key for Stability and Pathogenesis

Emily N. Gallichotte,[1,a] Kenneth H. Dinnon III,[1,a] Xin-Ni Lim,[2,3] Thiam-Seng Ng,[2,3] Elisa X. Y. Lim,[2,3] Vineet D. Menachery,[4,5] Shee-Mei Lok,[2,3,b] and Ralph S. Baric[1,4,b]

[1]Department of Microbiology and Immunology, University of North Carolina at Chapel Hill; [2]Program in Emerging Infectious Diseases, Duke-National University of Singapore Graduate Medical School; [3]Centre for BioImaging Science, National University of Singapore; [4]Department of Epidemiology, University of North Carolina at Chapel Hill; [5]Department of Microbiology and Immunology, University of Texas Medical Branch, Galveston

With severe disease manifestations including microcephaly, congenital malformation, and Guillain–Barré syndrome, Zika virus (ZIKV) remains a persistent global public health threat. Despite antigenic similarities with dengue viruses, structural studies have suggested the extended CD-loop and hydrogen-bonding interaction network within the ZIKV envelope protein contribute to stability differences between the viral families. This enhanced stability may lead to the augmented infection, disease manifestation, and persistence in body fluids seen following ZIKV infection. To examine the role of these motifs in infection, we generated a series of ZIKV recombinant viruses that disrupted the hydrogen-bonding network (350A, 351A, and 350A/351A) or the CD-loop extension (Δ346). Our results demonstrate a key role for the ZIKV extended CD-loop in cell-type-dependent replication, virion stability, and in vivo pathogenesis. Importantly, the Δ346 mutant maintains similar antigenicity to wild-type virus, opening the possibility for its use as a live-attenuated vaccine platform for ZIKV and other clinically relevant flaviviruses.

Keywords. Zika virus; structural virology; stability; cryo-electron microscopy; flavivirus.

Zika virus (ZIKV) is a flavivirus with a single-stranded positive-sense RNA genome of approximately 11 kb [1]. ZIKV is transmitted by *Aedes aegypti* and *Ae. albopictus* mosquitoes. It was first isolated in Uganda in 1947 [2] and caused sporadic outbreaks, mainly in Africa, Asia, and the South Pacific [3]. ZIKV has recently emerged as a global health threat after introduction to Brazil in 2015 and subsequent spread through South and Central America [4]. While ZIKV causes disease similar to related flaviviruses, infection is also associated with neurological pathologies like Guillain–Barré syndrome and meningoencephalitis [5], as well as fetal abnormalities such as microcephaly, placental insufficiency, and fetal demise [6, 7]. ZIKV has also been detected in fluids and tissues (tears, semen, testes, etc.) atypical of other flaviviruses, suggesting a unique pathobiology not common to other highly related viruses [8].

Like other flaviviruses, the surface of ZIKV is composed of the envelope protein (E), which is divided into three domains, domain I (EDI), II (EDII), and III (EDIII) [9]. Multiple cryo-electron microscopy (cryoEM) crystal structures found that the overall ZIKV structure is similar to dengue virus (DENV) and West Nile virus [9, 10], with subtle differences. The ZIKV E protein contains additional residues surrounding a glycosylation site in EDI, which might be important for attachment to host cells [9]. Additionally, the CD-loop in EDIII contains one additional amino acid relative to some other flaviviruses, allowing the loop to reach further into the 5-fold vertex (Figure 1A) [10]. This extended loop is predicted to augment ZIKV stability by facilitating a hydrogen-bond network among the five E monomers via a glutamine at position 350 of one molecule and a threonine at position 351 of the neighboring E molecule (Figure 1A) [10]. Multiple groups have since shown that mutating residue 350 and/or 351 has little to no impact on virus thermostability [11, 12]. These data suggest it is not the hydrogen-bonding within the CD-loop that leads to increased stability.

The extended CD-loop provides an alternative means of enhanced ZIKV stability, which is supported by reports that deletion of the CD-loop extension resulted in nonviable virus [12]. In this study, we used a H/PF/2013 ZIKV infectious clone [13] to generate a panel of viral mutants around the CD-loop. All viruses, including a residue 346 deletion (Δ346), were recovered and grew to high titer in multiple cell types. Consistent with prior reports, viruses with mutations designed to disrupt hydrogen-bonding (350A, 351A, and 350A/351A) showed no in vitro attenuation or decrease in thermostability. However, shortening the CD-loop by one amino acid attenuated the virus yields and led to a decrease in virus stability. Consonant with thermostability results, cryoEM analyses revealed that the deletion mutation (Δ346) destabilizes the virion, even at room

Received 28 May 2017; editorial decision 1 September 2017; accepted 6 September 2017; published online September 8, 2017.

[a]Authors contributed equally to this work.

[b]Co-senior authors.

Correspondence: Ralph S. Baric, PhD, 3304 Michael Hooker Research Building, CB #7435, Chapel Hill, NC 27599, USA (rbaric@email.unc.edu).

The Journal of Infectious Diseases® 2017;216:1196–204

DOI: 10.1093/infdis/jix473

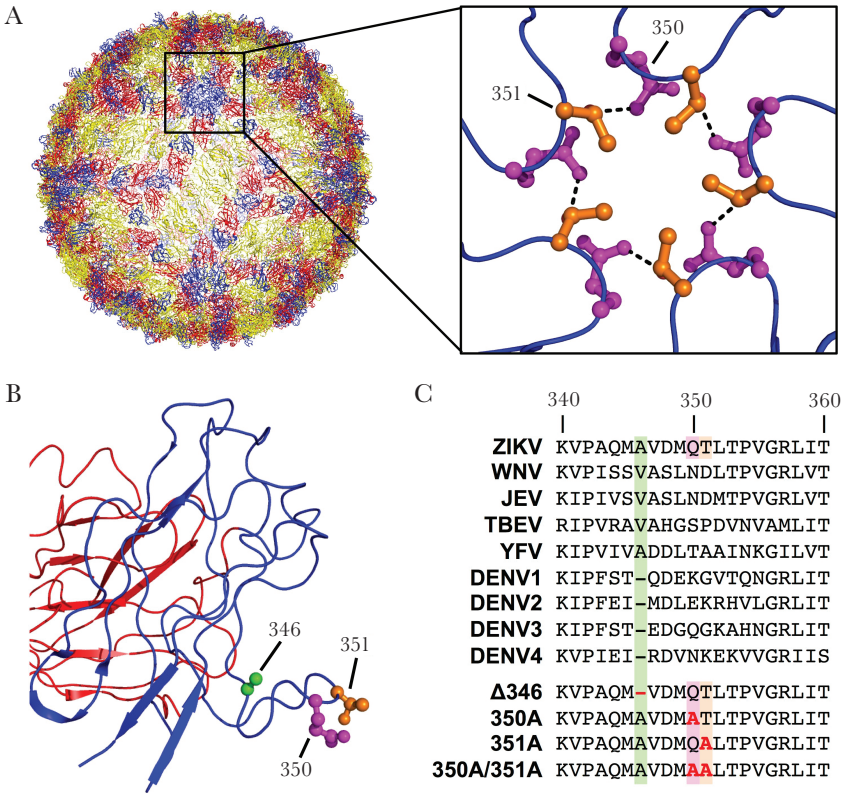

Figure 1. Zika virus (ZIKV) CD-loop and mutant virus design. *A*, The CD-loop of ZIKV contains a glutamine at position 350 and a threonine at position 351 and these residues are predicted to form a network of hydrogen bonds between the E proteins near the 5-fold vertex (Protein Data Bank = 5IZ7) [10]. *B*, Side view of CD-loop from a single envelope monomer. Residues 346, 350, and 351 that were altered in the CD-loop ZIKV mutant viruses are highlighted in green, magenta, and orange, respectively. *C*, Amino acid alignment of CD-loop region of ZIKV and related flaviviruses. Amino acid changes in mutant viruses are highlighted in red.

temperature. Importantly, all CD-loop mutant viruses maintained general ZIKV morphology and functional neutralizing antibody epitopes. In addition, the deletion mutant is attenuated in a mouse model of ZIKV disease. Overall, our data suggest that small changes in the ZIKV envelope improve stability and may play an important role in viral disease and pathogenesis.

METHODS

Viruses and Cells

Viruses were generated using our ZIKV H/PF/2013 reverse genetics infectious clone system [13]. Briefly, the viral genome was divided into four plasmids with unique type II restriction endonuclease sites at each end of the fragment. Fragments were digested, ligated together, in vitro transcribed, and electroporated into C6/36 cells. After incubating 4–6 days, cell culture supernatant was harvested, filtered to remove cellular debris, and passaged once on C6/36 cells to make a working stock.

To generate CD-loop mutant viruses, the following primers were used and polymerase chain reaction (PCR) was performed to introduce the mutations. Primer sequences listed 5′–3′ were: Δ346 forward (GTCAGAGTTTGCATGTCCACCATCTGAGC TGGAACCTTGC), Δ346 reverse (GTGGACATGCAAAC TCTGACC); 350A forward (ACTCTGACCCCAGTTGGGAG), 350A reverse (CTCCCAACTGGGGTCAGAGTTGCCATGT CCACCGCCATCTGAG); 351A forward (CTGACCCCAGTT GGGAGGTTG), 351A reverse (CAACCTCCCAACTGGGG TCAGAGCTTGCATGTCCACCGCCATCTGAG); and 350A/ 351A forward (ACTCTGACCCCAGTTGGGAG), 350A/ 351A reverse (CAACCTCCCAACTGGGGTCAGAGCTG CCATGTCCACCGCCATCTGAG). New plasmids containing CD-loop mutations were then digested and ligated as described above to make recombinant virus.

C6/36 cells (ATCC® CRL-1660) were maintained in Minimum Essential Medium, supplemented with 5% fetal bovine serum, 1% nonessential amino acids, and 1% antibiotic-antimycotic. Vero cells (ATCC® CCL-81) were maintained in Dulbecco's Modified Eagle Medium with 5% fetal bovine serum, and 1% antibiotic–antimycotic. Cells were cultured in 5% CO_2 at 37°C (Vero) or temperature-adapted to 32°C (C6/36).

Titering and Immunostaining

Viruses were serially diluted and added to approximately 80% confluent C6/36 or Vero cells. Diluted viruses were incubated on cells for 1 hour at 32°C (C6/36) or 37°C (Vero), then overlaid with 1% methylcellulose and incubated 4–5 days. Cells were

fixed with 50% methanol + 50% acetone and either stained with 0.25% crystal violet or immunostained with anti-E monoclonal antibody (MAb) 4G2.

Droplet Digital PCR

RNA was isolated from virus stocks using QIAGEN Viral RNA Isolation kit. Viral RNA was reverse-transcribed using Bio-Rad One-Step RT-ddPCR Kit for Probes and ddPCR Supermix, using the following primers and probe, listed 5′–3′: forward (GGATATTCAGGAACCCTGGC) reverse (AGTCCCACCTGACATACCTT), probe (GCAGCAGCTGCCATCGCTTGGCT) [14]. Droplets were generated and absolute genome copy numbers were determined using Bio-Rad QX200 Droplet Digital PCR System [15].

Growth Curves

C6/36 or Vero cells were infected in triplicate at a multiplicity of infection (MOI) of either 0.01 or 1, for 1 hour at 32°C (C6/36) or 37°C (Vero). After incubation, wells were washed with PBS to remove unbound virus, and fresh growth media was added to wells. Every 6–24 hours, culture supernatant was removed, immediately frozen at −80°C, then titered as described above. Cells were washed, fixed in 10% formalin, permeabilized, and stained with anti-E MAb 4G2 conjugated to AlexaFluor 488. Infected cells were quantified using flow cytometery (Guava® easyCyte, Millipore).

Temperature Stability Assay

For temperature-dependent stability assay, virus stocks were diluted 1:10 and incubated at either 4°C, 28°C, 37°C, or 40°C for 8 hours. Viruses were immediately titered as described above. For temperature time course assay, viruses were diluted 1:10 and incubated at 37°C. Samples were removed at various time points, immediately frozen at −80°C, and subsequently titered together as described above. Relative infectivity was determined as (focus forming units [FFU]/$mL_{test\ temperature}$/FFU/$mL_{4°C}$) × 100 for temperature-dependent assay, and (FFU/$mL_{time\ indicated}$/FFU/$mL_{t=0h}$) × 100 for time-dependent assay.

Cryo-Electron Microscopy

Viruses were prepared as previously described [10, 16]. Briefly, viruses were grown in C6/36 cells, precipitated in polyethylene glycol, pelleted by ultracentrifugation, purified through a sucrose cushion, then purified in a potassium tartrate gradient. Virus samples were incubated at 4°C, 29°C, 37°C, or 40°C for 30 minutes then frozen onto copper cryoEM grids. Micrograph images were collected on a Titan Krios (FEI) microscope.

Binding Enzyme Linked Immunosorbent Assay

Ninety-six well plates were coated with mouse anti-E MAb 4G2 overnight at 4°C. Plates were blocked with 3% nonfat dried milk, and viruses were captured. Primary human MAb C10 was diluted and added to wells, then goat-α-human-IgG alkaline phosphatase (AP) labeled secondary antibody was added. Plates were developed with *p*-nitrophenyl phosphate substrate, and color changes were quantified by spectrophotometry.

Monoclonal Antibody Focus Reduction Neutralization Test

Human MAb C10 was diluted 4-fold starting at 10ng/μL and mixed with approximately 50 FFU of virus, and MAb:virus mixture was incubated at 32°C for 1 hour. MAb:virus mixture was added to approximately 80% confluent C6/36 cells and incubated an additional hour at 32°C. After incubation, 1% methylcellulose overlay was added to cells, and plates were incubated 4 days. Cells were fixed and stained as described above.

Mouse Infections

Male and female 11-week-old type I and type II interferon receptor knockout mice ($IFNAR^{-/-}$ $IFNGR^{-/-}$) on C57BL/6 background were provided from Jason Whitmire at University of North Carolina, and were infected with 10^3 C6/36 FFU in 10μL via a footpad injection. Survival and weight loss were monitored daily across a 28-day period. At day 6 post-infection, a subset of mice were euthanized, sera and brains were collected and immediately stored at −80°C. Sera and brain homogenates were titered as described. Animals were humanely euthanized upon dropping below 80% of their starting weight or showed signs of disease. All animal work was performed in adherence to the Institutional Animal Care and Use Committee (IACUC) and University of North Carolina at Chapel Hill policy.

RESULTS

Design of Zika Virus CD-Loop Mutants

To investigate the role of ZIKV's extended CD-loop and potential inter-envelope hydrogen-bonding, we designed a panel of CD-loop mutants using a ZIKV H/PF/2013 infectious clone (Figure 1) [13]. Relative to DENV, but similar to other flaviviruses (Figure 1C), ZIKV contains an additional amino acid in the CD-loop at position 346, allowing the loop to reach farther into the 5-fold vertex (Figure 1A and B) [10]. To determine the impact of the extended loop, we generated a recombinant virus (Δ346) removing the alanine at position 346 (Figure 1C). To study the impact of inter-envelope hydrogen-bonding between glutamine at position 350 and threonine at position 351 across neighboring molecules (Figure 1B), we individually or together mutated these resides to alanine to disrupt these interactions (350A, 351A, and 350A/351A, respectively) (Figure 1C). CD-loop mutants were generated using an infectious clone and recovered in C6/36 cells.

Characterizing CD-Loop Mutants

Viral stocks grown on C6/36 cells indicated roughly equivalent levels of genome copies, suggesting similar virus-packaging of genomes (Supplementary Figure 1A). When titered on C6/36 cells, 350A, 351A, and 350A/351A mutant titers were similar

to WT ZIKV, whereas Δ346 was approximately 1 log attenuated (Figure 2A). Titering the same stocks on Vero cells showed a similar pattern, where 350A, 351A, and 350A/351A mutant titers were similar to WT ZIKV; however, Δ346 was attenuated by 2 logs (Figure 2B). This difference was also highlighted in a higher genome to FFU ratio for the Δ346 mutant in Vero cells (Supplementary Figure 1B). Additionally, the ratio of Vero titer to C6/36 titer showed that WT ZIKV, 350A, 351A, and 350A/351A had 1/10th the infectious virus on Vero cells relative to C6/36 cells, whereas Δ346 had 1/100th the amount (Supplementary Figure 1C). To determine whether this difference in ratio in the Δ346 mutant is cell-type dependent or due to different culture temperatures of C6/36 and Vero cells (32°C or 37°C, respectively), we titered viruses on Vero cells at both temperatures. Independent of incubation temperature, WT ZIKV, and Δ346 titers did not change (Supplementary Figure 1D), suggesting cell-type dependent attenuation of mutant Δ346.

While CD-loop mutants make viral foci similar to those of WT ZIKV in C6/36 cells, Δ346 foci were substantially smaller than those of WT ZIKV in Vero cells (Figure 2C), in contrast to the 350A, 351A, and 350A/351A mutants. Additionally, Δ346 did not plaque in Vero cells after the standard 4 days of incubation, requiring additional time (5–7 days) to generate small plaques (Supplementary Figure 2). These data suggest that Δ346 mutant is attenuated in cell-to-cell spread in Vero cells, whereas the other mutants show no attenuation.

CD-Loop Mutant Replication

To extend our analysis of mutant virus growth, we performed growth curves to evaluate replication attenuation. In a multistep growth curve (MOI = 0.01) on C6/36 cells, Δ346 was slightly attenuated relative to WT ZIKV and reached significantly lower peak titer (Figure 3A), despite similar levels of infected cells (Supplementary Figure 3A). At a higher MOI of 1, all viruses had similar replication kinetics; however, Δ346 still reached a significantly lower peak titer (Figure 3A, Supplementary Figure 3A). More robust attenuation of Δ346 was observed in Vero cells at early times in both low and high MOIs ($P < .01$); however, the Δ346 mutant eventually reached a similar peak titer (Figure 3B). Interestingly, the Q350A and T351A single and double mutants appeared to be enhanced in growth relative to WT virus in multicycle growth curves in both cell types (Figure 3A and B). Disrupting CD-loop hydrogen-bonding interactions potentially improves virus entry, fusion, assembly, or egress, leading to an improved growth of these viruses. Together, the peak titer and multistep growth curve data indicate a critical early role for the extended CD-loop in ZIKV replication and propagation, which differs between cell types.

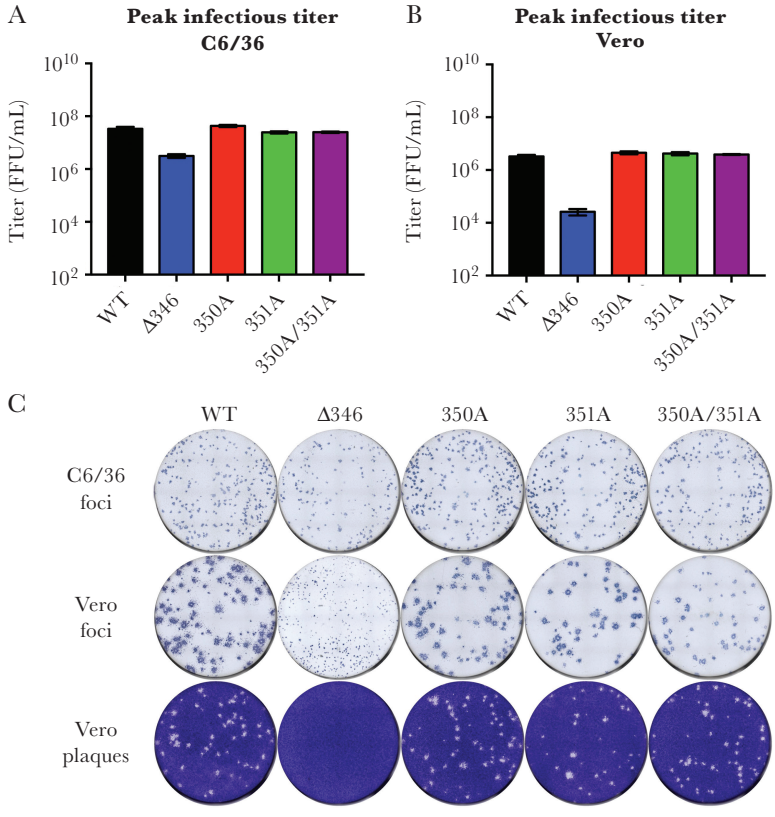

Figure 2. Recovery of infectious CD-loop mutants. *A,B*, The focus forming units (FFU) (mean ± standard deviation) of the virus stocks were determined on (*A*) C6/36 and (*B*) Vero cells. *C*, Viruses were titered on C6/36 or Vero cells and immunostained with anti-E MAb 4G2, or crystal violet. WT, wild type.

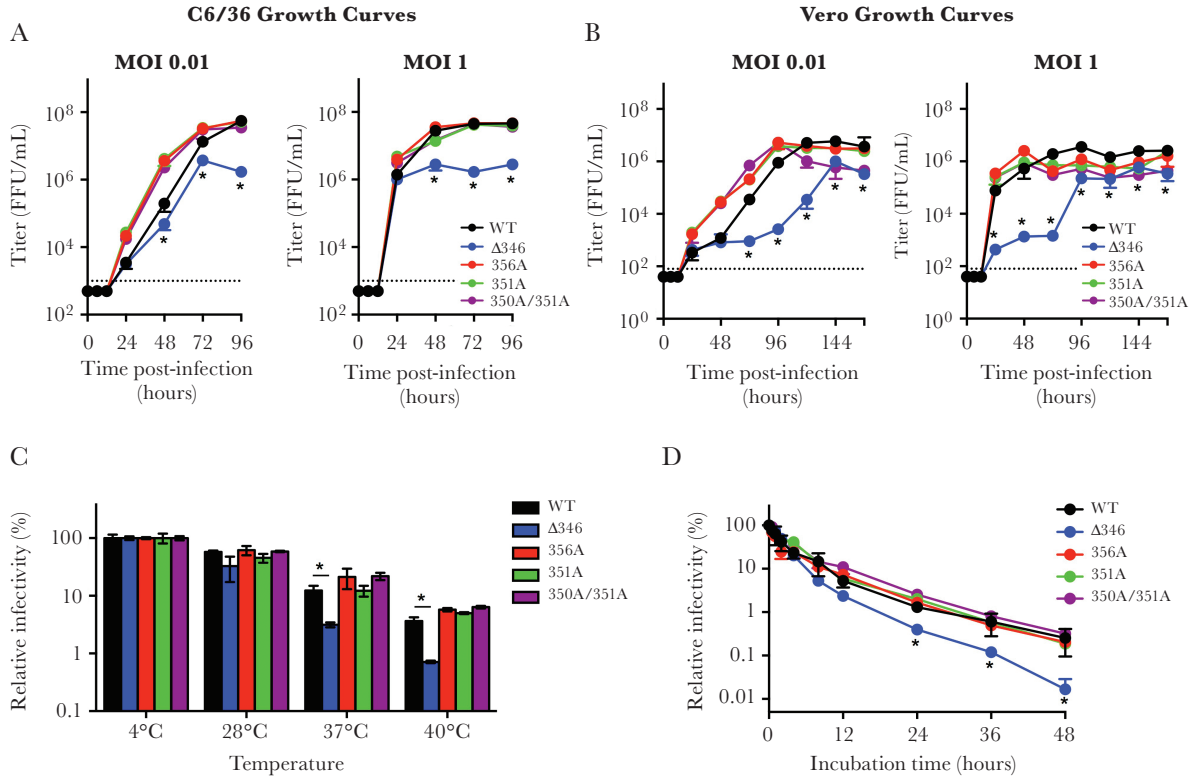

Figure 3. Δ346 mutant is attenuated in growth and thermally unstable. Growth curves of wild type (WT) and mutant viruses in (*A*) C6/36 cells or (*B*) Vero cells. *C*, Thermal stability of viruses that were incubated at 4°C, 28°C, 37°C, or 40°C for 8 hours, and then titered on C6/36 cells. Relative infectivity was calculated as (focus forming units [FFU]/$mL_{test\ temperature}$/FFU/$mL_{4°C}$) × 100 (mean ± standard error of the mean [SEM]). *D*, Infectivity of viruses when incubated for various timings at 37°C. Relative infectivity was calculated as (FFU/$mL_{time\ indicated}$/FFU/$mL_{t=0h}$) × 100 (mean ± SEM). One-way analysis of variance followed by Dunnett's multiple comparisons test was conducted on log-transformed data (*$P < .05$). Dotted lines represent limit of detection.

Δ346 Mutation Disrupts Virus Temperature Stability

To explore if changes in virus stability reduced viral replication, the mutant viruses were incubated at a range of temperatures and subsequently titered on C6/36 cells. For all viruses, similar stability was observed at both 4°C and 28°C (Figure 3C). However, the Δ346 mutant had significantly reduced infectivity ($P < .05$) at both 37°C and 40°C relative to WT ZIKV as well as the 350A, 351A, and 350A/351A mutants (Figure 3C). Extending this analysis, we examined intrinsic decays of each virus at the physiologically relevant temperature 37°C, and sampled over the course of 48 hours. While WT ZIKV, 350A, 351A, and 350A/351A all decayed at similar rates, the Δ346 mutant lost infectivity significantly ($P < .01$) faster at this temperature (Figure 3D). Together, the data argue that reduced temperature stability might contribute to the attenuation of the Δ346 mutant.

Shortening the CD-Loop Destabilizes Virus

The CD-loop mutants were designed to disrupt inter-envelope interactions at the 5-fold vertex on the intact virion, by either shortening the CD-loop (Δ346) or disrupting hydrogen bond interactions (350A, 351A, and 350A/351A). The temperature stability results suggest that the extended CD-loop rather than the hydrogen bond interactions are critical for ZIKV thermostability (Figure 3C and D). To determine if the Δ346 mutant has reduced overall stability, cryoEM was performed on the Δ346 and other CD-loop mutants. CyroEM micrographs indicate that WT ZIKV is structurally stable even up to 40°C, maintaining primarily spherical virion morphology (Figure 4), consistent with previous work [10]. Interestingly, even at 4°C, the Δ346 mutant is highly unstable with only a small fraction of particles appearing spherical (Figure 4). Increasing the incubation temperature of the viruses after cryoEM virus purification did not appear to increase the instability of the virus or the fraction of broken particles. It is possible that the Δ346 is breaking apart during the virus preparation and ultracentrifugations for cryoEM, and therefore any additional manipulations after this preparation did not further impact stability. Consistent with growth and temperature stability results (Figure 3), 350A, 351A, and 350A/351A mutants looked similar to WT ZIKV (Figure 4), with temperature having little impact. These results suggest that modification of the ZIKV CD-loop reduces the stability of the virion and may impact viral replication and propagation.

Mutant Viruses Maintain Zika Virus Morphology and Neutralizing Antibody Epitopes

While alteration of E protein residues has produced viable DENV mutants [17–19], manipulation of the CD-loop may

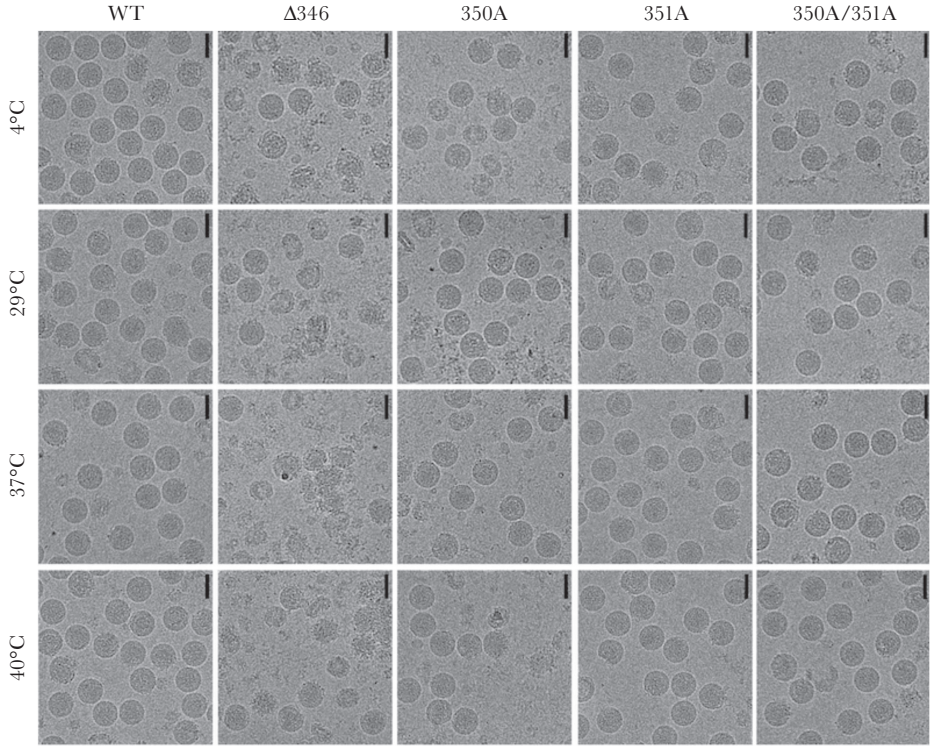

Figure 4. Deletion mutation at the ZIKV CD-loop leads to structural instability. CryoEM micrographs of wild type (WT) and CD-loop mutant virus particles after incubation at 4°C, 29°C, 37°C, and 40°C for 30 minutes. Scale bar is 50 nm.

result in disrupted ZIKV virion morphology, antigenic presentation, and contribute to reduced thermostability. To ensure conservation of important ZIKV neutralizing epitopes, we evaluated each mutant for the ability to bind C10, an envelope dimer epitope (EDE) cross-reactive DENV antibody [16, 20, 21]. Each CD-loop mutant bound C10 with similar kinetics to WT ZIKV (Figure 5A). Importantly, the epitope was not only maintained in mutant viruses, but also retained the ability to be neutralized by C10 with similar neutralization titers (Figure 5B). Importantly, infectious virus produced by cells used in binding and neutralization assays, maintained this functional epitope, corroborating that the structural instability of Δ346 seen in cryoEM micrographs is instead likely due to the strenuous preparation process for cyroEM analyses, including multiple ultracentrifugations. Overall, these results suggest that despite modification of the CD-loop, ZIKV antigenicity remained intact.

Δ346 is Attenuated in a Mouse Model of Zika Virus Pathogenesis

To determine the impact of thermoinstability of the Δ346 mutant on in vivo pathogenesis, we utilized a mouse model of ZIKV infection and pathogenesis [22]. Using 11-week-old type I and type II interferon receptor knockout mice, we infected with 10^3 FFU WT ZIKV or Δ346 and followed these mice over a 28-day time course.

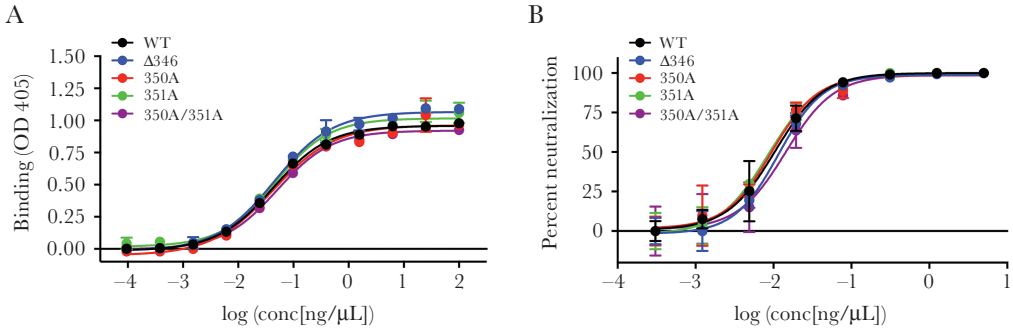

Figure 5. CD-loop mutants maintain Zika virus antigenicity. *A*, Enzyme-linked-immunosorbent-assay and (*B*) focus reduction neutralization test (FRNT) was performed with all virus stocks and dengue virus monoclonal antibody (DENV MAb) EDE1 C10 to determine levels of antibody binding and neutralization (mean ± SD).

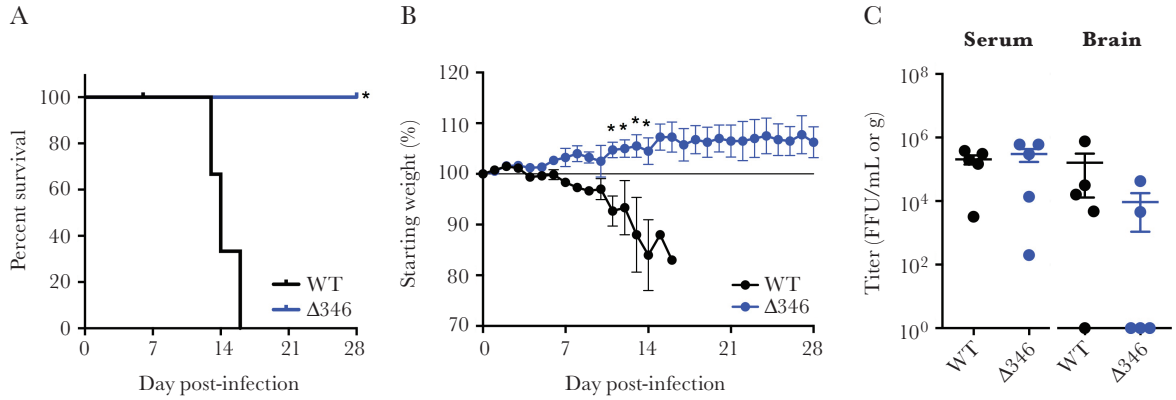

Figure 6. Δ346 mutant is attenuated in a mouse model of Zika virus disease. *A–C*, Eleven-week old type I/II interferon receptor knockout mice were infected with 10^3 C6/36 focus forming units via footpad injection and monitored for (*A*) survival (log-rank test, $^*P < .05$) and (*B*) weight loss (mean ± standard error of the mean [SEM]) (two-tailed Student *t* test, $^*P < .05$). *C*, Mice were harvested at day 6, and serum and brain were collected and titered on C6/36 cells (mean ± SEM). Virus below limits of detection are plotted on x axis. WT, wild type.

All mice infected with WT ZIKV succumbed to disease by day 16 (Figure 6A), with weight loss beginning day 7 postinfection (Figure 6B). Conversely, infection with Δ346 resulted in no significant disease or weight loss (Figure 6A and B). To confirm productive infection of each virus, serum virus titer was measured at day 6. Surprisingly, mice infected with either WT ZIKV or the Δ346 mutant had comparable serum viremia (Figure 6C). At the same time-point however, fewer mice infected with Δ346 had detectable virus in their brain, and those with virus had lower titer virus than those infected with WT ZIKV (Figure 6C). These results suggest that attenuation of the Δ346 mutant in mice is not primarily due to lack of replicating virus early during infection, but might be due to trafficking to, or replication in, the brain.

DISCUSSION

In this study, we examined the role of ZIKV's extended CD-loop and potential hydrogen-bonding interactions on virus stability using a series of structurally designed mutants. Despite initial predictions [10], disrupting the hydrogen bond interactions through three different mutations (350A, 351A, and 350A/351A) had little to no impact on virus titer, replication, stability, or structural morphology. Combined with previous reports, these results show that the predicted hydrogen-bonding across envelope proteins at the 5-fold vertex is not primarily responsible for ZIKV's thermostability [11, 12]. In contrast, removing a single residue from the ZIKV CD-loop led to a decrease in virus titer, foci size, ability to plaque in Vero cells, and thermostability. While a previous study argued the extended CD-loop is essential for ZIKV assembly as they were unable to recover virus from electroporated Vero cells [12], electroporation into the more permissive C6/36 cells allowed recovery of the Δ346 mutant, suggesting cell-type-dependent viability or differences in the efficiencies of recovering debilitated mutants in the two molecular clone systems. Additionally, the Δ346 mutant was attenuated in a mouse model of ZIKV disease, with lower titer in the brain and decreased pathogenesis. Importantly, while shortening the CD-loop maintained general ZIKV morphology and neutralizing antibody epitopes, it also disrupted virion structural stability, consistent with temperature stability results. It is possible that maturation state and or differences in sensitivity to pH changes might also impact mutant virus stability. Together, the results confirm a significant role for the extended CD-loop in ZIKV infection and pathogenesis.

These results illustrate the utility of mechanistic validation of structural predictions. While initial analyses indicated a role for hydrogen-bonding in the ZIKV CD-loop leading to enhanced stability, these and other studies have now shown that preventing these hydrogen-bonding interactions has little impact on stability [11, 12]. In contrast, our data provide direct evidence that the CD-loop extension is at least partially responsible for enhanced stability. Notably, ZIKV has been detected in fluids and tissues (tears, semen, testes, etc.) not seen with the related DENV strains, which maintain a shorter CD-loop [8]. One possibility is that ZIKV's extended CD-loop provides a thermo- and structural stability advantage that permits persistence, travel to organs and fluids atypical of the related DENVs [23]. Importantly, conservation of the extended CD-loop in other flaviviruses, including West Nile and yellow fever viruses (YFV), may signal this modification as a possible correlate for pathogenesis; mutation of these loops in other flaviviruses may render similar attenuation as seen with the Δ346 mutant. While the YFV vaccine was heavily passaged to attenuate the virus, the mechanism of attenuation is still poorly understood and vaccination occasionally results in adverse side effects, especially in the elderly [24–28]. While speculative, it is possible shortening the CD-loop of the YFV vaccine may further attenuate the virus and lead to better tolerability.

In addition to loss of virion stability and in vitro attenuation, the Δ346 mutant also demonstrated in vivo attenuation.

Infection with the CD-loop mutant produced minimal weight loss, the absence of lethality, and diminished brain titers in type I/II IFN receptor knockout mice. Importantly, despite the structural instability, the CD-loop mutant maintains similar antigenicity to WT ZIKV based on antibody binding and neutralization by the envelope-dimer epitope antibody. With future availability of additional ZIKV-specific monoclonal antibodies, more thorough analysis can be performed to evaluate CD-loop mutant virus morphology, presentation of epitopes, and antigenicity. These results indicate that the Δ346 mutation could serve as a backbone for a live attenuated vaccine platform [29]. However, further studies, including examination of persistence in peripheral tissues, antibody/protection responses, possibility for reversion, and potential mosquito transmission, are still required. Notably, based on conservation across other flaviviruses, manipulation of the CD-loop extension may have implication beyond ZIKV for vaccine design.

In the context of an outbreak, varying research approaches must work in concert to develop both understanding and therapeutic interventions. While epidemiological studies provide critical insights, they are inherently limited by the quality of reporting and surveillance in the epidemic setting [30]. Similarly, rapid publication of ZIKV cryoEM structures [9, 10] allowed predictions of factors that influence the emerging infection, but could not test those observations. In this study, we have leveraged a newly developed ZIKV infectious clone [13] to explore and test insights from structure based studies. The resulting rationally designed mutants confirmed the importance of the CD-loop extension, but not hydrogen-bonding, in ZIKV stability. Importantly, the approach to integrate these diverse strategies can be applied to newly emerging viruses to elucidate mechanisms of pathogenesis and design next-generation therapeutics.

Supplementary Data

Supplementary materials are available at *The Journal of Infectious Diseases* online. Consisting of data provided by the authors to benefit the reader, the posted materials are not copyedited and are the sole responsibility of the authors, so questions or comments should be addressed to the corresponding author.

Notes

Previous presentation. This work was previously presented at the Gordon Research Conference, Viruses and Cells (May 2017, Lucca, Italy) and the 2017 American Society of Virology meeting (June 2017, Madison, Wisconsin).

Funding. This research was supported by funding from R01 AI107731 (principal investigator, Aravinda de Silva), U19 AI109761 and AI107810 programs (R. S. B), Singapore Ministry of Education Tier 3 grant (MOE2012-T3-1–008), National Research Foundation Investigatorship Award (NRF-NRFI2016-01), National Research Foundation Competitive Research Project Grant (NRF2016NRF-CRP001-063), and the Duke-NUS Signature Research Programme funded by the Ministry of Health, Singapore, awarded to S. M. L. Training grant funding T32 AI1007419 from the US National Institute of Allergy and Infectious Diseases supported E. N. G.

Potential conflicts of interest. All authors: No reported conflicts of interest. All authors have submitted the ICMJE Form for Disclosure of Potential Conflicts of Interest. Conflicts that the editors consider relevant to the content of the manuscript have been disclosed.

References

1. Wang A, Thurmond S, Islas L, Hui K, Hai R. Zika virus genome biology and molecular pathogenesis. Emerg Microbes Infect **2017**; 6:e13.
2. Dick GW, Kitchen SF, Haddow AJ. Zika virus. I. Isolations and serological specificity. Trans R Soc Trop Med Hyg **1952**; 46:509–20.
3. Wikan N, Smith DR. Zika virus: history of a newly emerging arbovirus. Lancet Infect Dis **2016**; 16:e119–26.
4. Paixão ES, Barreto F, Teixeira Mda G, Costa Mda C, Rodrigues LC. History, epidemiology, and clinical manifestations of Zika: A Systematic Review. Am J Public Health **2016**; 106:606–12.
5. Li H, Saucedo-Cuevas L, Shresta S, Gleeson JG. The neurobiology of Zika virus. Neuron **2016**; 92:949–58.
6. Rasmussen SA, Jamieson DJ, Honein MA, Petersen LR. Zika virus and birth defects–reviewing the evidence for causality. N Engl J Med **2016**; 374:1981–7.
7. Coyne CB, Lazear HM. Zika virus - reigniting the TORCH. Nat Rev Microbiol **2016**; 14:707–15.
8. Miner JJ, Diamond MS. Zika virus pathogenesis and tissue tropism. Cell Host Microbe **2017**; 21:134–42.
9. Sirohi D, Chen Z, Sun L, et al. The 3.8 Å resolution cryo-EM structure of Zika virus. Science **2016**; 352:467–70.
10. Kostyuchenko VA, Lim EX, Zhang S, et al. Structure of the thermally stable Zika virus. Nature **2016**; 533:425–8.
11. Goo L, Dowd KA, Smith AR, Pelc RS, DeMaso CR, Pierson TC. Zika virus is not uniquely stable at physiological temperatures compared to other flaviviruses. mBio **2016**; 7:e01396–16.
12. Xie X, Yang Y, Muruato AE, et al. Understanding Zika virus stability and developing a chimeric vaccine through functional analysis. mBio **2017**; 8: e02134–16.
13. Widman DG, Young E, Yount BL, et al. A reverse genetics platform that spans the Zika virus family tree. mBio **2017**; 8:e02014–16.
14. Lanciotti RS, Kosoy OL, Laven JJ, et al. Genetic and serologic properties of Zika virus associated with an epidemic, Yap State, Micronesia, 2007. Emerg Infect Dis **2008**; 14:1232–9.
15. Hindson BJ, Ness KD, Masquelier DA, et al. High-throughput droplet digital PCR system for absolute quantitation of DNA copy number. Anal Chem **2011**; 83:8604–10.

16. Zhang S, Kostyuchenko VA, Ng TS, et al. Neutralization mechanism of a highly potent antibody against Zika virus. Nat Commun **2016**; 7:13679.
17. Gallichotte EN, Menachery VD, Yount BL, Jr, et al. Epitope addition and ablation via manipulation of a dengue virus serotype 1 infectious clone. mSphere **2017**; 2: e00380–16.
18. Gallichotte EN, Widman DG, Yount BL, et al. A new quaternary structure epitope on dengue virus serotype 2 is the target of durable type-specific neutralizing antibodies. mBio **2015**; 6:e01461–15.
19. Messer WB, Yount BL, Royal SR, et al. Functional transplant of a Dengue virus serotype 3 (DENV3)-specific human monoclonal antibody epitope into DENV1. J Virol **2016**; 90:5090–7.
20. Swanstrom JA, Plante JA, Plante KS, et al. Dengue virus envelope dimer epitope monoclonal antibodies isolated from dengue patients are protective against Zika virus. mBio **2016**; 7:e01123–16.
21. Barba-Spaeth G, Dejnirattisai W, Rouvinski A, et al. Structural basis of potent Zika-dengue virus antibody cross-neutralization. Nature **2016**; 536:48–53.
22. Lazear HM, Govero J, Smith AM, et al. A mouse model of Zika virus pathogenesis. Cell Host Microbe **2016**; 19:720–30.
23. Hirsch AJ, Smith JL, Haese NN, et al. Zika virus infection of rhesus macaques leads to viral persistence in multiple tissues. PLoS Pathog **2017**; 13:e1006219.
24. Collins ND, Barrett AD. Live attenuated yellow fever 17D vaccine: a legacy vaccine still controlling outbreaks in modern day. Curr Infect Dis Rep **2017**; 19:14.
25. Barrett AD. Yellow fever live attenuated vaccine: A very successful live attenuated vaccine but still we have problems controlling the disease. Vaccine **2017**; doi: 10.1016/j.vaccine.2017.03.032.
26. Khromava AY, Eidex RB, Weld LH, et al.; Yellow Fever Vaccine Safety Working Group. Yellow fever vaccine: an updated assessment of advanced age as a risk factor for serious adverse events. Vaccine **2005**; 23:3256–63.
27. Lindsey NP, Rabe IB, Miller ER, Fischer M, Staples JE. Adverse event reports following yellow fever vaccination, 2007–13. J Travel Med **2016**; 23. doi: 10.1093/jtm/taw045.
28. Monath TP, Cetron MS, McCarthy K, et al. Yellow fever 17D vaccine safety and immunogenicity in the elderly. Hum Vaccin **2005**; 1:207–14.
29. Barouch DH, Thomas SJ, Michael NL. Prospects for a Zika virus vaccine. Immunity **2017**; 46:176–82.
30. Lilienfeld AM. Practical limitations of epidemiologic methods. Environ Health Perspect **1983**; 52:3–8.